ISSN 0965-5441, Petroleum Chemistry, 2022, Vol. 62, No. 7, pp. 779–787. © The Author(s), 2022. This article is an open access publication.
Russian Text © The Author(s), 2022, published in Neftekhimiya, 2022, Vol. 62, No. 5, pp. 691–700.

V-Containing Heteropoly Acids with Keggin Structure as Precursors of Sulfide Catalysts: Regularities of the Convertion of Dibenzothiophene and Naphthalene on Nonpromoted Mo–V Catalysts

V. V. Timoshkina[a,*], S. V. Yudintsev[a], E. D. Frenkel'[a], and A. A. Pimerzin[a,b]

[a] *Samara State Technical University, Samara, 443100 Russia*
[b] *OOO Gazpromneft – Industrial Innovations, St. Petersburg, 197350 Russia*
**e-mail: aquariusviktoria@mail.ru*

Received April 7, 2022; revised May 24, 2022; accepted June 8, 2022

Abstract—Mixed PMoV heteropoly acids with Keggin structures $H_{3+x}PMo_{12-x}V_xO_{40}$ (x = 1–6) and modified sulfide catalysts on their basis were synthesized, their physicochemical characteristics were determined, and their performance in the reactions of hydrodesulfurization (HDS) of dibenzothiophene (DBT) and hydrogenation of naphthalene was evaluated. Modification of the Mo-containing catalysts with vanadium by impregnation with a solution of mixed heteropoly acids was found to enhance their catalytic activity in the studied reactions, as well as to increase the selectivity for the direct hydrodesulfurization route of the DBT HDS reaction.

Keywords: hydrodesulfurization, hydrogenation, dibenzothiophene, heteropoly acids, molybdenum, vanadium

DOI: 10.1134/S0965544122050085

Catalytic hydroprocessing is one of the most important current technologies in petroleum refining industry, which allows removing undesirable, e.g., sulfur-containing compounds from petroleum fractions and obtaining commercial products of better quality [1]. Continuous tightening of environmental requirements for motor fuels requires constant optimization of existing hydrotreatment technologies, which problem is most logically handled by catalyst improvement. There is a need in development of new catalytic systems affording hydrogenates with ultralow sulfur content, even if the quality of the feedstock deteriorates [2].

Heteropoly compounds (HPCs) are a class of inorganic compounds with diversified molecular structures, possessing a broad range of properties, which find application in various fields of science such as chemistry, biology, medicine, and materials science and, in particular, are used in catalysis [3]. Numerous studies have been focused on the redox and acid properties of HPCs, which are directly related to their composition. The most popular are HPCs with Keggin structures which, owing to stability and facile preparation, have been extensively used as active phase precursors for hydrotreating catalysts over several decades [2]. The structural form of α-Keggin anions having the general formula $[XM_{12}O_{40}]^{n-}$, where X is a heteroatom (most often, P^{5+}, Si^{4+}, or B^{3+}), and M is the addendum atom (most commonly, Mo and W), self-assembles in an acidic aqueous solution and represents the most stable structure of polyoxometalate catalysts [4].

Modern hydrotreating catalysts typically include Co(Ni) and Mo(W) compounds supported on γ-Al_2O_3 from water-soluble salts such as, e.g., ammonium molybdate and nickel nitrate [5]. It has been repeatedly demonstrated that replacement of conventional precursors by Mo(W)-containing HPCs improves the catalytic performance of hydrotreating catalysts [6–8]. The diversity of HPC structures and compositions enables synthesis of complexes containing both atoms of the main active elements and of the promoter elements by varying their ratios [9]. Another route to increasing the activity of hydrotreating catalysts involves the use of inorganic

modifiers [10]. One effective approach to improving the catalytic performance involves the use of Co(Ni)XMoS mixed sulfides, where X is a d metal [11].

The latest published data indicate that modification with small amounts of vanadium increases the activity of hydrotreating catalysts [12–15]. The catalytic activity can be enhanced by using: vanadium as a modifying additive [12], complex metal compositions [13], HPCs as active phase precursors [14], an alternative activation method [15], etc.

Herein, a combination of two methods of improving the performance of the catalysts was implemented via synthesizing mixed HPCs comprising not only the active metal, Mo, but also the modifier metal, V.

The aim of this study was to synthesize sulfide catalysts based on V-containing Keggin HPCs and to examine their physicochemical characteristics and catalytic properties, as well as to compare the efficiencies of the synthesized and conventional catalysts in dibenzothiophene hydrodesulfurization and naphthalene hydrogenation reactions.

EXPERIMENTAL

Complex acids whose anion is constituted by two different acidic oxides (PMoV HPAs) of the composition $H_{3+x}PMo_{12-x}V_xO_{40}$ with Keggin structure (where x = 1, 2, 3, 4, 5, 6) were synthesized according to the procedure described in [16]. In the first stage, V_2O_5 is dissolved in a cooled H_2O_2 solution to obtain peroxovanadium compounds, which then spontaneously decompose to form an $H_6V_{10}O_{28}$ solution. The latter is stabilized by addition of H_3PO_4, yielding an $H_9PV_{14}O_{42}$solution which is added to a boiling $H_3PO_4 + MoO_3$ aqueous suspension; during its evaporation MoO_3 gradually dissolves, forming a PMoV HPA solution. The resulting 0.2 M solution is concentrated by evaporation to give a concentrate which is used for preparation of an impregnating solution.

PMoV catalysts were prepared by single incipient wetness impregnation of the support (γ-Al_2O_3) with a solution of HPA having the appropriate composition. Reference samples were synthesized on the basis of phosphomolybdic acid and ammonium metavanadate. After impregnation the samples were dried at temperatures of 60 and 80°C for 2 h and at 110°C for 6 h. The choice of the contents of the active metals was dictated by relevant published data and the results of our studies [17, 18]. The metal content in the catalysts synthesized was monitored by X-ray fluorescence (XRF) spectrometry using a Shimadzu EDX800HS analyzer.

The textural characteristics of the prepared catalysts were analyzed by low-temperature nitrogen adsorption–desorption on a Quantachrome Autosorb-1 porosimeter. The specific surface area of the catalysts was determined using the Brunauer–Emmett–Teller (BET) model at a relative partial pressure P/P_0 = 0.05–0.3; the total pore volume and the pore diameter distribution were calculated using the Barrett–Joyner–Halenda model.

The structure of the HPAs synthesized was confirmed by X-ray diffraction and Fourier- transform IR spectroscopy. X-ray diffraction patterns were obtained on a Rigaku SmartLab device using CuK_α radiation (λ = 1.54 Å, scan speed 2 deg/min) in the 2θ range from 5° to 70°. The IR spectra of the HPA samples were measured in the range of 400–4000 cm^{-1} on an IRTracer-100 (Shimadzu) instrument with an ATR (attenuated total internal reflection) accessory.

The temperature-programmed reduction analysis of the PMoV samples was performed using a TPDRO 1100 (Thermo Scientific) device under the following conditions: temperature from room temperature to 600°C, heating rate 10°C/min, flow rate of the argon-hydrogen mixture 30 mL/min, hydrogen concentration in the argon-hydrogen mixture 5 vol %.

The catalytic properties of the mixed samples were investigated on a catalytic fixed-bed flow laboratory setup. The reactor was loaded with 0.9 cm^3 of the catalyst particles 0.25–0.50 mm in size. The catalysts were subjected to gas-phase sulfidation treatment at 400°C and 1 MPa in an H_2S/H_2 (10/90 vol %) atmosphere for 2.5 h. A model mixture of DBT (0.86 wt %), naphthalene (3.0 wt %) in toluene with n-hexadecane (1.0 wt %) added as an internal standard served as a feedstock. The catalyst activity was examined under the following conditions: temperature range 320–360°C, hydrogen pressure in the system 3.0 MPa, liquid hourly space velocity 4.5–9 h^{-1}, and volume ratio of H_2 to the feedstock 600 nL/L. The hydroconversion process was carried out for at least 8 h after a stable conversion of the reactant was attained.

The composition of the liquid products mixture sampled every hour was determined chromatographically on a Crystal-5000 instrument equipped with a flame ionization detector and a OV-101 nonpolar column (stationary phase dimethylpolysiloxane 30 m × 0.5 mm × 0.5 μm).

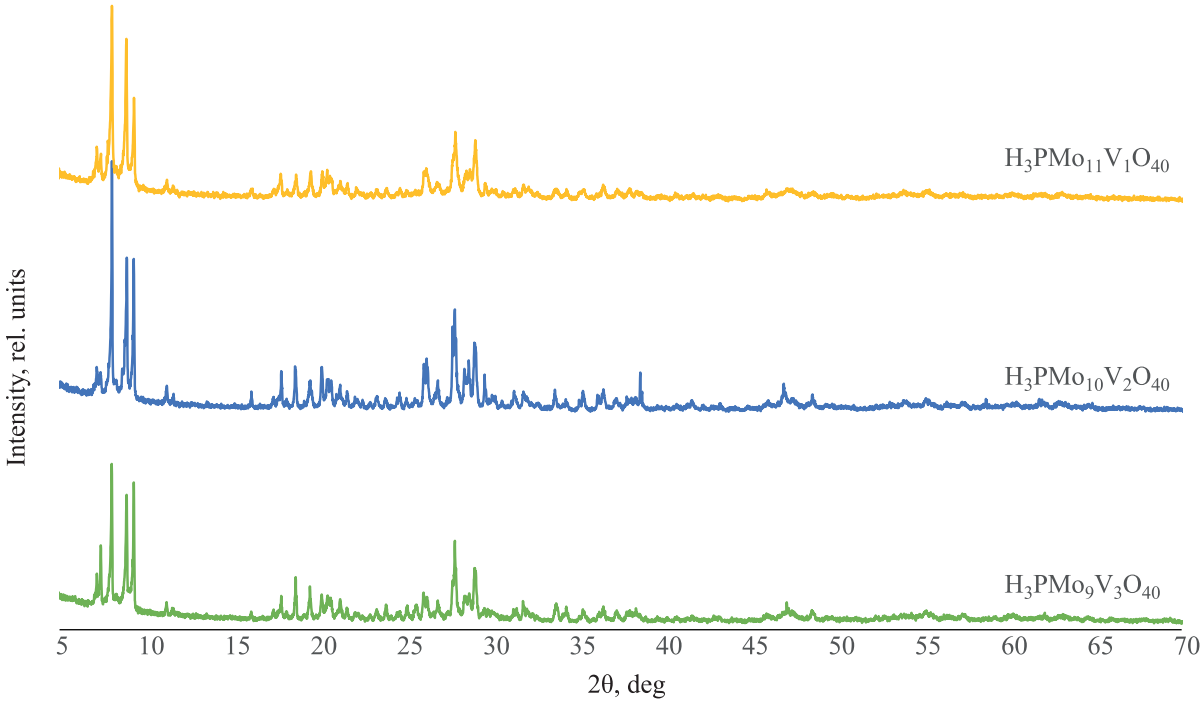

Fig. 1. X-ray diffraction patterns of the synthesized HPAs.

The activity of the catalyst in the hydrodesulfurization and hydrogenation reactions was estimated from the apparent reaction rate constant calculated using the pseudo-first-order kinetic model equation:

$$k = -\frac{F}{W}\ln(1-x), \quad (1)$$

where F is the reactant (DBT, naphthalene) flow rate, mol/h, W, weight of MoO_3, g, and x, reactant conversion, %.

Also, the relative selectivity of the DBT HDS reaction for direct desulfurization and pre-hydrogenation routes was evaluated. The relative selectivity (Sel) was calculated as the ratio of the total concentration of the products obtained by the direct hydrogenation route, i.e., of tetrahydrodibenzothiophene (THDBT), dicyclohexyl (DCH), and cyclohexylbenzene (CHB), to the concentration of biphenyl (BP) produced from the DBT molecule via direct desulfurization route:

$$\mathrm{Sel}_{\mathrm{HYD/HDS}} = \frac{C_{\mathrm{CHB}} + C_{\mathrm{DCH}} + C_{\mathrm{THDBT}}}{C_{\mathrm{BP}}}, \quad (2)$$

where C_{CHB}, C_{DCH}, C_{THDBT}, and C_{BP} are the respective concentrations of cyclohexylbenzene, dicyclohexyl, tetrahydrodibenzothiophene, and biphenyl.

The apparent activation energy E_a was estimated using the Arrhenius equation, i.e., the experimentally determined temperature dependence of ln k.

RESULTS AND DISCUSSION

Figure 1 shows the X-ray diffraction patterns of selected HPAs synthesized with the composition $H_{3+x}PMo_{12-x}V_xO_{40}$ (x = 1, 2, 3). The most significant X-ray diffraction peaks of the PVMo HPAs are observed in the 2θ ranges of 7°–10°, 18°–23°, and 25°–30°. Upon addition of vanadium the crystallinity and the main diffraction peaks in the 2θ range from 5° to 35° are preserved. According to the literature, the X-ray diffraction patterns of phosphomolybdic acid exhibit well-defined peaks; hence, the Keggin anion structure remains virtually unchanged upon incorporation of one vanadium atom [19].

The heteropoly anions formed can be identified by characteristic IR bands in the range of 850–1100 cm^{-1}, which were observed in the spectra of a series of the vanadium-containing HPAs. The absorption bands at 1043–1055 cm^{-1} are attributable to the vibrations of the

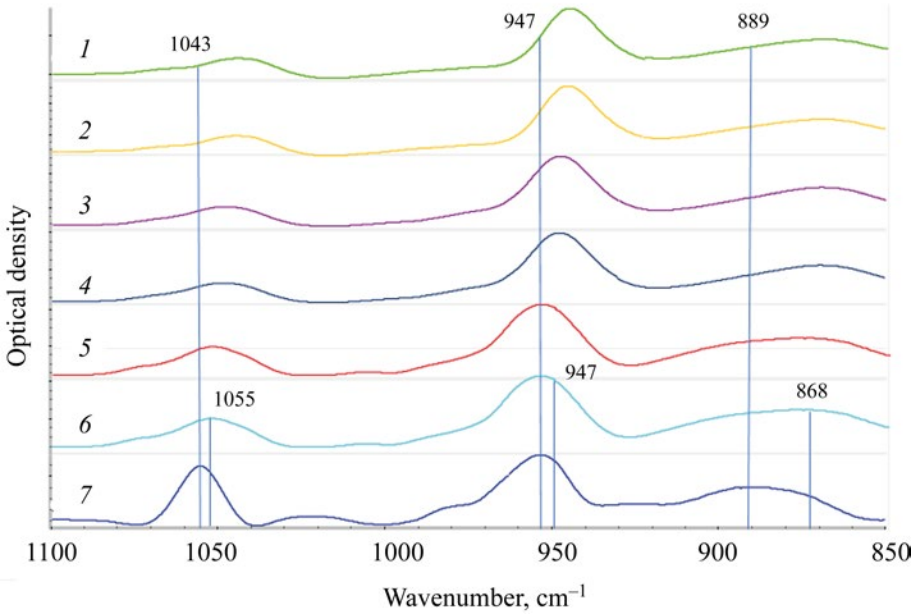

Fig. 2. IR spectra of the synthesized HPAs: (*1*–*6*) $H_{3+x}PMo_{12-x}V_xO_{40}$ (x = 1–6) and (*7*) $H_3PMo_{12}O_{40}$.

P–O bonds, and those at 947–955 cm^{-1}, to M(Mo,V)=O bonds. In the range of 868–889 cm^{-1} there are also bands associated with the vibrations of the bridging M–O–M bonds. Figure 2 shows that, with an increase in the number of the vanadium atoms in the $H_{3+x}PMo_{12-x}V_xO_{40}$ molecule, each IR band in the spectra of the series of the prepared HPAs was shifted towards lower wavenumbers, in agreement with the published data [20].

Table 1 presents the composition and the textural characteristics of the synthesized catalysts in the oxide form, and Figs. 3 and 4, the corresponding nitrogen adsorption–desorption isotherms and pore size distributions.

Impregnation of the support with the HPA solution leads to decreases in the specific surface area (from 309 to 249–277 m^2/g) and in the pore volume (from 0.83 to 0.60–0.71 cm^3/g), whereas the pattern of the pore size distribution is preserved (Fig. 4). The nitrogen adsorption–desorption curves for the support and the catalyst samples exhibit a type-IV profile characteristic of mesoporous materials (Fig. 3).

Table 1. Characteristics of the support and the series of the catalysts in the oxide form

Catalyst (sample)	Content, wt %		Textural characteristics		
	MoO_3	V_2O_5	S_{BET}, m^2/g	V_{pore}, cm^3/g	D_{max}[a], nm
Al_2O_3	–	–	309	0.83	7.3/13.0
PMo_{12}	13.0	–	249	0.64	6.3/11.4
PV_1Mo_{11}	13.2	0.9	252	0.62	6.0/11.7
PV_2Mo_{10}	14.8	2.1	234	0.62	5.2/11.7
PV_3Mo_9	13.4	2.8	267	0.66	6.0/11.6
PV_4Mo_8	10.6	3.6	270	0.70	6.5/11.7
PV_5Mo_7	8.8	4.4	277	0.71	5.2/11.6
PV_6Mo_6	8.5	7.8	267	0.68	5.2/11.6
PV_{12}	–	21.6	255	0.60	5.6/12.3

[a] Maximum in the pore size distribution curve (Fig. 4).

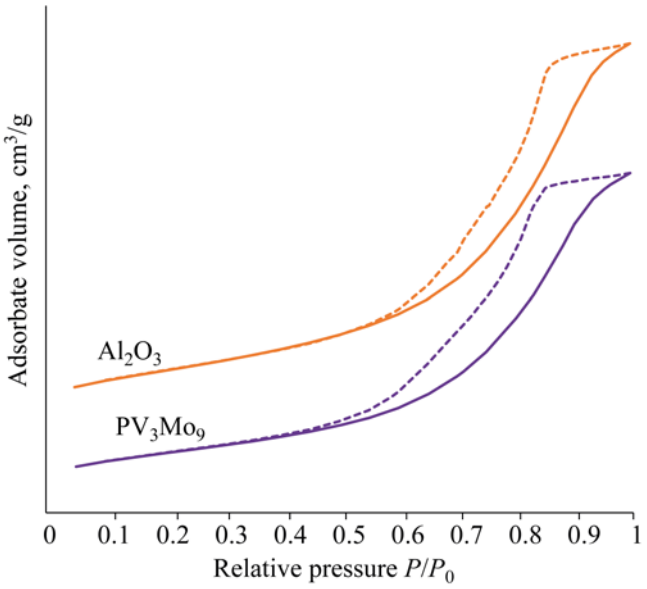

Fig. 3. Nitrogen adsorption–desorption curves at 77 K for the support and the catalysts.

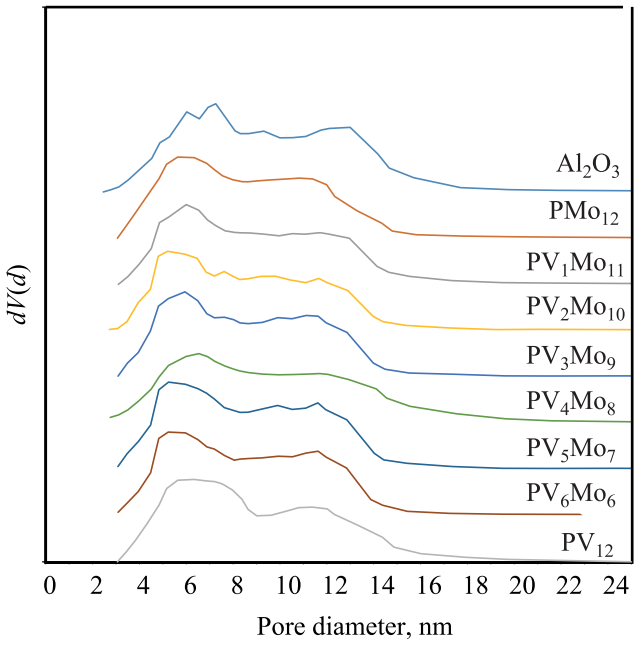

Fig. 4. Pore size distribution curves for the support and the catalysts.

The amount of vanadium loaded on the catalyst affects the TPR patterns exhibited by the samples of the catalyst in the oxide form (Fig. 5). The reduction of all the studied samples begins at a temperature of 400–420°C, with the intensity of the TPR peak of the catalysts increasing as $PMo_{12} < PV_6Mo_6 < PV_{12}$ within the temperature range of 490–550°C. Also, an increase in the V loading on the catalyst causes the amount of the hydrogen consumed under the reducing conditions to increase.

Incorporation of V into the catalyst composition significantly affects the TPR patterns (Fig. 6) recorded for the sulfide catalysts. The onset of reduction of the sulfides of all the studied samples is observed at a temperature of 200–220°C. Vanadium loading causes shifting of the TPR peak of the catalysts in the PMo_{12}–V_2Mo_{10}–PV_6Mo_6 series within the temperature range of 320–350°C toward higher values, while the V amount has little effect on the final temperature. The TPR peak area also increases upon

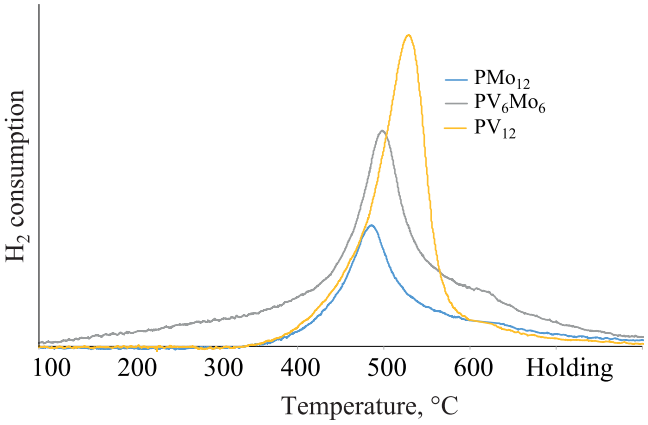

Fig. 5. Temperature-programmed reduction curves of the samples of the catalysts in the oxide form.

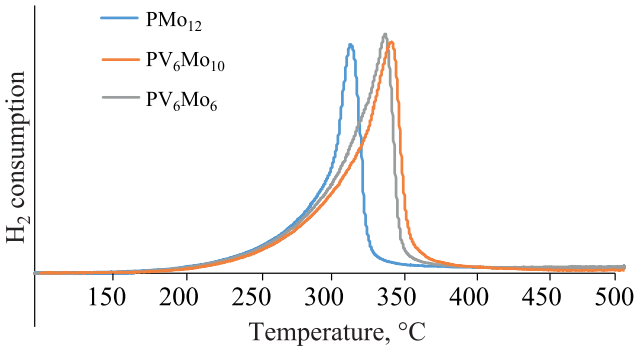

Fig. 6. Temperature-programmed reduction curves of the samples of the catalyst in the sulfide form.

Table 2. Results of the catalytic tests

Liquid hourly space velocity, LHSV	Catalyst							
	PMo_{12}	PV_1Mo_{11}	PV_2Mo_{10}	PV_3Mo_9	PV_4Mo_8	PV_5Mo_7	PV_6Mo_6	PV_{12}
DBT conversion 320°C, %								
4.5 h^{-1}	23.2	36.1	40.9	43.5	37.9	38.3	30.3	–
9 h^{-1}	10.8	19.6	23.4	23.9	19.0	17.6	18.4	5.6
DBT conversion 340°C, %								
4.5 h^{-1}	43.9	57.3	60.1	60.1	46.4	53.8	63.0	35.4
9 h^{-1}	25.5	36.4	37.7	40.7	25.5	35.5	33.6	16.4
DBT conversion 360°C, %								
4.5 h^{-1}	59.1	–	69.6	64.0	57.0	57.5	69.4	60.0
9 h^{-1}	39.3	51.7	48.7	46.0	39.2	40.3	47.9	36.8
13.5 h^{-1}	25.4	–	35.7	35.4	27.2	30.5	32.6	–
Naphthalene conversion 320°C, %								
4.5 h^{-1}	40.4	52.3	54.6	54.8	49.4	50.3	43.0	–
9 h^{-1}	24.5	34.8	38.9	38.2	27.8	26.8	41.0	7.5
Naphthalene conversion 340°C, %								
4.5 h^{-1}	58.3	65.5	64.9	64.7	56.1	61.1	65.8	42.7
9 h^{-1}	39.4	50.2	50.7	50.9	37.2	45.9	43.0	24.7
Naphthalene conversion 360°C, %								
4.5 h^{-1}	64.4	–	66.8	62.0	58.3	60.5	66.5	50.8
9 h^{-1}	49.5	59.2	56.2	51.2	45.3	47.8	53.3	36.6
13.5 h^{-1}	38.3	–	46.8	43.8	33.8	38.4	40.4	–

vanadium incorporation, suggesting an increase in the number of the metal sulfide-based active sites.

Table 2 presents the range of the conversions of dibenzothiophene and naphthalene under the experimental conditions. For the series of the catalyst samples the DBT conversion at a temperature of 320°C is in the range of 5.6–43.5%, that at 340°C, in the range of 16.4–63.0%, and that at 360°C ranges from 25.4 to 69.6%. The naphthalene conversion at a temperature of 320°C is in the 7.5–54.8% range, that at 340°C, in the 24.7–65.8% range, and that at 360°C ranges from 33.8 to 66.8%. The PV_{12} reference catalyst is characterized by low conversions of the reactants.

Figures 7 and 8 demonstrate the changes in the catalytic activity exhibited by the samples in dibenzothiophene hydrogenolysis and naphthalene hydrogenation reactions. The rate constants of both reactions tend to increase as the vanadium loading in the precursor increases. For the DBT hydrogenolysis reaction at a temperature of 320°C the reaction rate constant increases in the range of 6.7–17.3, that at 340°C, in the range of 15.0–37.1, and that at 360°C, in the range of 23.2–49.0 mol $g_{MoO_3}^{-1}$ h^{-1}. The rate constant of the reaction of naphthalene hydrogenation at a temperature of 320°C increases in the range of 70.9–127.0, that at 340°C, in the range 126.7–216.0, and that at 360°C, in the range of 173.6–299.1 mol $g_{MoO_3}^{-1}$ h^{-1}. It should be noted that, with increasing temperature, the reaction rate constants display a more pronounced increase. The reference catalyst PV_{12} showed low catalytic activity.

Changes in E_a for the Mo-containing catalysts occur in a narrow range (54.7–97.5 kJ/mol for the DBT HDS reaction, and 44.7–77.6 kJ/mol for the naphthalene HYD reaction), as seen from Fig. 9. With an increase in the V loading on the samples the apparent activation energies

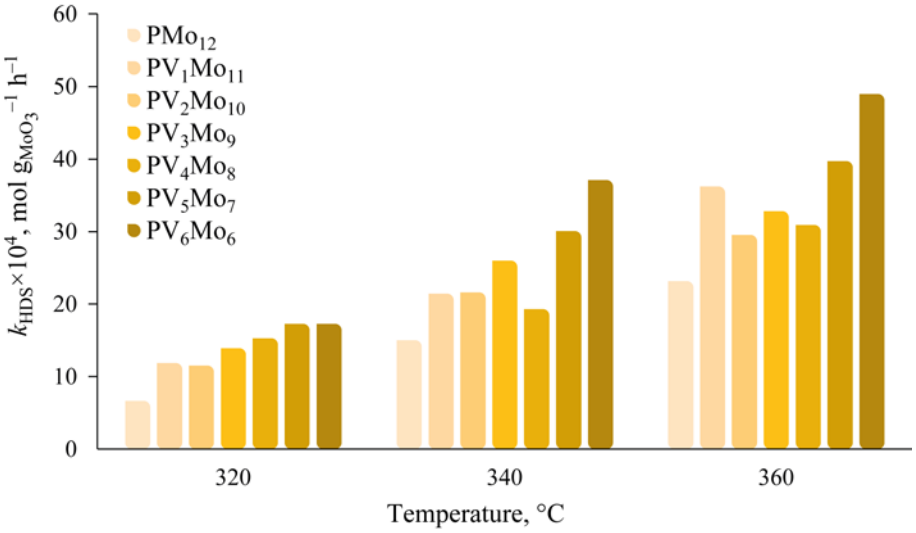

Fig. 7. Rate constant on the MoO_3 weight basis for the DBT HDS reaction at $T = 320$, 340, and 360°C.

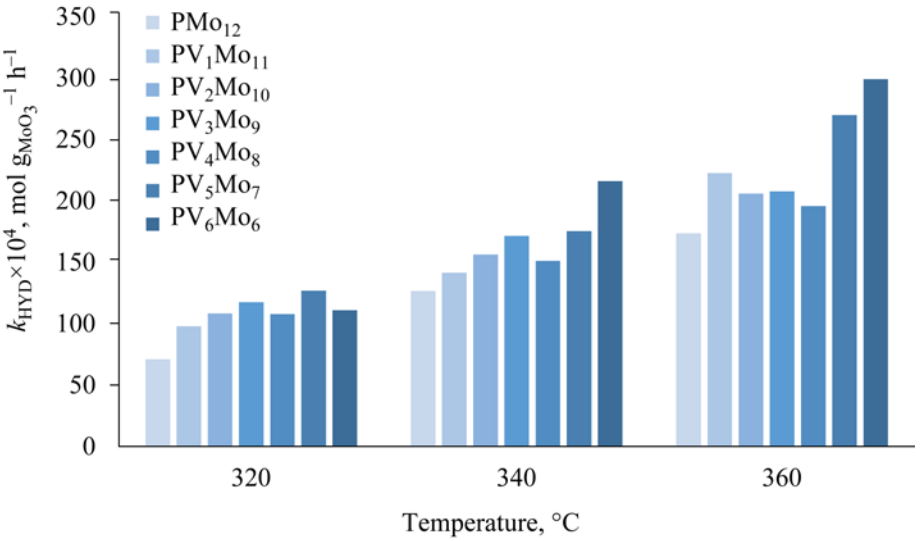

Fig. 8. Rate constant on the MoO_3 weight basis for the naphthalene HYD reaction at $T = 320$, 340, and 360°C.

of the HDS and HYD reactions tend to decrease. It is likely that the active sites on the modified catalyst samples are more energetically favorable to allow the model reactions. The lowest E_a values in the DBT HDS reaction are exhibited by the catalysts with 3 to 5 V atoms, and in the naphthalene HYD reaction, by those with 2 to 4 V atoms. For the V-based catalyst sample (without MoO_3) E_a is significantly higher, which may be due to different mechanisms of the reactions considered.

Incorporation of vanadium into the catalyst composition alters the DBT HDS reaction route selectivity (Table 3). With an increase in the V loading on the catalyst the relative reaction rate along the direct desulfurization route tends to increase; $Sel_{HYD/HDS}$ decreases from 2.66 for PMo_{12} to 1.16 for PV_6Mo_6 catalyst at 320°C, from 2.35 to 1.31 at 340°C, and from 1.59 to 0.83 at 360°C. The change in the reaction route selectivity is indicative of the alteration of the catalytic properties of the active phase (number and ratio of the active sites for hydrogenation and desulfurization routes) of the catalysts, caused by V incorporation into their composition. Low selectivity

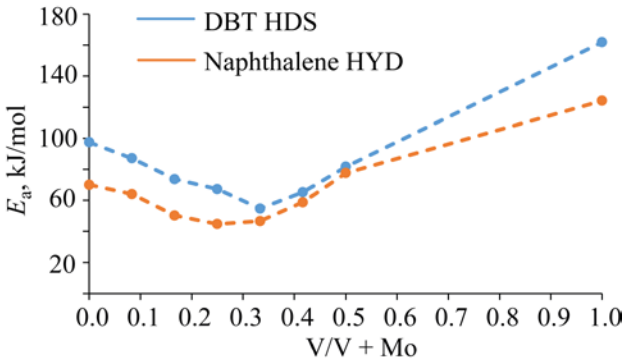

Fig. 9. Activation energies of the DBT HDS and the naphthalene HYD reactions in relation to the amount of vanadium loaded on the catalysts.

of the V-based catalyst compared to the MoV analogs deserves menttioning.

CONCLUSIONS

The present study demonstrated the efficiency of V incorporation into the composition of the molybdenum catalyst from the synthesized HPC. The resultant catalysts exhibit enhanced hydrogenation and hydrodesulfurization activities as compared to the initial molybdenum-based catalyst, as well as lower selectivities in the hydrogenation and desulfurization reactions.

In general, this line of research holds promise for studying modified catalytic systems. The results from these studies may be useful in development of new highly active catalysts to be applied in existing technologies for hydrotreatment of petroleum fractions.

Table 3. Selectivity of the DBT HDS reaction for the pre-hydrogenation route [Eq. (2)] in relation to the V loading

Catalyst	$Sel_{HYD/HDS}$		
	320°C	340°C	360°C
PMo_{12}	2.66	2.35	1.59
PV_1Mo_{11}	2.27	1.84	–
PV_2Mo_{10}	2.47	1.89	1.38
PV_3Mo_9	1.73	1.99	0.88
PV_4Mo_8	1.43	1.12	0.77
PV_5Mo_7	1.53	1.25	0.84
PV_6Mo_6	1.16	1.31	0.83
PV_{12}	–	0.84	0.57

AUTHOR INFORMATION

V.V. Timoshkina, ORCID: https://orcid.org/0000-0002-1373-2476

S.V. Yudintsev, ORCID: https://orcid.org/0000-0002-2736-5785

E.D. Frenkel', ORCID: https://orcid.org/0000-0001-7524-1544

A.A. Pimerzin, ORCID, https://orcid.org/0000-0003-1578-5106

CONFLICT OF INTEREST

The authors declare no conflict of interest requiring disclosure in this article.

OPEN ACCESS

REFERENCES

1. de León, J.N.D., Kumar, C.R., Antúnez-García, J., and Fuentes-Moyado, S., *Catalysts*, 2019, vol. 9, no. 1, pp. 1–26. https://doi.org/10.3390/catal9010087
2. Weng, X., Cao, L., Zhang, G., Chen, F., Zhao, L., Zhang, Y., Gao, J., and Xu, C., *Ind. Eng. Chem. Res*., 2020, vol. 59, no. 49, pp. 21261–21274. https://doi.org/10.1021/acs.iecr.0c04049.
3. Misono, M., *Stud. Surf. Sci. Catal*., 2013, vol. 176, pp. 97–155. https://doi.org/10.1016/B978-0-444-53833-8.00004-1
4. Pope, M.T., in *Comprehensive Coordination Chemistry II: Transition Metal Groups 3–6*, Wedd, A.G., Ed., New York: Elsevier, 2004, pp. 644–650.
5. North, J., Poole, O., Alotaibi, A., Bayahia, H., Kozhevnikova, E.F., Alsalme, A., Siddiqui, M.R.H., and Kozhevnikov, I.V., *Appl. Catal., A: General*, 2015, vol. 508, pp. 16–24. https://doi.org/10.1016/j.apcata.2015.10.001

6. Tanimu, A. and Alhooshani, K., *Energy Fuels*, 2019, vol. 33, no. 4, pp. 2810–2838. https://doi.org/10.1021/acs.energyfuels.9b00354
7. Griboval, A., Blanchard, P., Payen, E., Fournier, M., and Dubois, J.L., *Catal. Today*, 1998, vol. 45, nos. 1–4, pp. 277–283. https://doi.org/10.1016/S0920-5861(98)00230-2
8. Lizama, L. and Klimova, T., *Appl. Catal., B: Environ*., 2008, vol. 82, nos. 3–4, pp. 139–150. https://doi.org/10.1016/j.apcatb.2008.01.018
9. Okuhara, T., Mizuno, N., and Misono, M., *Adv. Catal*., 1996, vol. 41, pp. 113–252. https://doi.org/10.1016/S0360-0564(08)60041-3
10. Berhault, G., in *New Materials for Catalytic Applications*, Parvulescu, V.I. and Kemnitz, E., Eds., New York: Elsevier, 2016, vol. 10, pp. 313–360. https://doi.org/10.1016/B978-0-444-63587-7.00010-X
11. Afanasiev, P. and Bezverkhyy, I., *Appl. Catal., A: General*, 2007, vol. 322, pp. 129–141. https://doi.org/10.1016/j.apcata.2007.01.015
12. Soogund, D., Lecour, P., Daudin, A., Guichard, B., Legens, C., Lamonier, C., and Payen, E., *Appl. Catal., B: Environ*., 2010, vol. 98, nos. 1–2, pp. 39–48. https://doi.org/10.1016/j.apcatb.2010.04.024
13. Betancourt, P., Marrero, S., and Pinto-Castilla, S., *Fuel Process. Technol.*, 2013, vol. 114, pp. 21–25. https://doi.org/10.1016/j.fuproc.2013.03.013
14. Betancourt, P., Rives, A., Scott, C.E., and Hubaut, R., *Catal. Today*, 2000, vol. 57, pp. 201–207.
15. Janssens, J.P., van Langeveld, A.D., and Moulijn, J.A., *Appl. Catal., A: General*, 1999, vol. 179, nos. 1–2, pp. 229–239. https://doi.org/10.1016/S0926-860X(98)00319-6
16. Odyakov, V.F., Zhizhina, E.G., Rodikova, Y.A., and Gogin, L.L., *Eur. J. Inorg. Chem*., 2015, vol. 2015, no. 22, pp. 3618–3631. https://doi.org/10.1002/ejic.201500359
17. Sun, M., Adjaye, J., and Nelson, A.E., *Appl. Catal., A: General*, 2004, vol. 263, no. 2, pp. 131–143. https://doi.org/10.1016/j.apcata.2003.12.011
18. Solmanov, P.S., Maksimov, N.M., Tomina, N.N., Eremina, Y.V., Timoshkina, V.V., Pimerzin, A.A., and Verevkin, S.P., *Russ. J. Appl. Chem*., 2018, vol. 91, no. 8, pp. 1363–1369. https://doi.org/10.1134/S096554411902018X
19. Barats-Damatov, D., Shimon, L.J.W., Feldman, Y., Bendikov, T., and Neumann, R., *Inorg. Chem*., 2015, vol. 54, no. 2, pp. 628–634. https://doi.org/10.1021/ic502541b
20. Park, D.R., Kim, H., Jung, J.C., Lee, S.H., and Song, I.K., *Catal. Commun*., 2008, vol. 9, no. 2, pp. 293–298. https://doi.org/10.1016/j.catcom.2007.06.025